

## Smart Polymer Surfaces

**Spiros H. Anastasiadis**,<sup>\*,†,‡</sup> **Haris Retsos**,<sup>†,‡,⊥</sup> **Stergios Pispas**,<sup>§</sup>  
**Nikos Hadjichristidis**,<sup>\*,§</sup> and **Stylianos Neophytides**<sup>||</sup>

*Institute of Electronic Structure and Laser, Foundation for Research and Technology—Hellas, P.O. Box 1527, 711 10 Heraklion Crete, Greece, Department of Physics, University of Crete, 710 03 Heraklion Crete, Greece, Department of Chemistry, University of Athens, 15771 Zografou Athens, Greece, and Institute of Chemical Engineering and High-Temperature Processes, Foundation for Research and Technology—Hellas, 26500 Rion Patras, Greece*

*Received July 15, 2002*

**ABSTRACT:** A methodology is demonstrated for creating responsive polymer surfaces that can alter their wetting characteristics when exposed to a humid environment. For this, we take advantage of the surface partitioning of block copolymers at the polymer/air interface and utilize a hydrophilic group at the end of the surface-active block. When exposed to water vapor, the end group, hidden below the surface when in contact with dry air, presents itself to the surface thus significantly reducing the water contact angle. This function can be reversed and repeated again and again by successive exposures of the surface to dry and wet environment, respectively.

### I. Introduction

The properties of material surfaces/interfaces are of fundamental importance in scientific areas such as wetting, lubrication, tackiness, and adhesion, which control a variety of applications in, e.g., biotechnology, industrial coatings, cosmetics, etc.<sup>1</sup> The wettability of a solid material is controlled by its surface energy: when a liquid is in contact with a solid surface in static equilibrium with its vapor, the liquid may form a contact angle  $\theta$  with the surface (partial wetting) when the various surface tensions obey Young's equation

$$\gamma_{LV} \cos \theta = \gamma_{SV} - \gamma_{SL} \quad (1)$$

where  $\gamma_{SV}$  is the surface tension of the solid,  $\gamma_{LV}$  that of the liquid, and  $\gamma_{SL}$  the solid–liquid interfacial tension. For complete wetting,  $\gamma_{SV} - \gamma_{SL} \geq \gamma_{LV}$ , with the equal sign signifying zero contact angle. Therefore, wetting is promoted for high substrate surface tension  $\gamma_{SV}$ , low fluid surface tension  $\gamma_{LV}$ , and/or low solid–liquid interfacial tension  $\gamma_{SL}$ , whereas dewetting is favored in the opposite limits.

Tailoring the wettability of a surface is being attempted by various means of surface modification. Deposition of self-assembled monolayers (SAM's) produces terminally attached organic modifiers,<sup>2–4</sup> whose terminus functional moieties determine the hydrophobicity/hydrophilicity of the final surface by decreasing/increasing the material surface energy. Recently, mechanically assembled monolayers<sup>5</sup> were utilized in order to create superhydrophobic polymer surfaces. External physicochemical treatments<sup>6</sup> (e.g., oxygen plasma or ultraviolet/ozone or corona discharge) are frequently used to increase the surface polarity. The above proce-

dures, however, require an extra processing step for the modification of the material surface. Moreover, when high-energy surfaces are created by these means, they usually deteriorate with time due to surface reconstruction. Alternatively, low energy surfaces (oleophobic or hydrophobic) can be prepared by the addition of interfacially active components, which selectively segregate to the interface in order to reduce the total free energy of the system. Therefore, a need emerges for the creation of hydrophilic surfaces using additives and without extra processing steps. These additives should be able to express hydrophilicity by responding to external stimuli.

In recent years, various efforts have been presented for the development of materials that can respond to environmental stimuli, such as changes in pH, temperature, or the presence of a specific chemical substrate, where the emphasis was on switchability and reversibility. Hydrogels, which swell or shrink in response to environmental changes, find applications as biomaterials and drug-delivery systems<sup>7</sup> whereas complex patterns are generated on their surfaces.<sup>8,9</sup> Synthesis of hybrid materials, which combine two different types of properties (e.g., hydrogels with colloidal crystals<sup>10,11</sup> or with coiled-coil proteins<sup>12</sup>) can lead to systems exhibiting temperature- or chemical-sensing properties. Concerning surfaces, utilization of a fluorinated polymer liquid crystal coating in the temperature range of a smectic-to-isotropic bulk phase transition produced a switchable surface with respect to both wettability and tack.<sup>13</sup> Moreover, changes in temperature of an oxidized polymer in water affected its wettability,<sup>14</sup> whereas the influence of surface heterogeneity, cooperativity and dynamics on the responsiveness of a polymer surface has been discussed.<sup>15</sup> When an ordered amphiphilic diblock copolymer film is soaked in a selective solvent, a different microdomain is observed at the free surface.<sup>16</sup> A polystyrene-*block*-poly(methyl methacrylate) brush synthesized on a solid surface<sup>17</sup> presents a different block to the surface when immersed in a selective solvent whereas a binary brush made of end-anchored incompatible homopolymers responds to a selective solvent due to the swelling of one polymer and the

\* To whom correspondence should be addressed.

† Institute of Electronic Structure and Laser, Foundation for Research and Technology—Hellas.

‡ University of Crete.

§ University of Athens.

|| Institute of Chemical Engineering and High-Temperature Processes, Foundation for Research and Technology—Hellas.

⊥ Present address: Department of Materials, University of California at Santa Barbara, Santa Barbara, CA 93106.

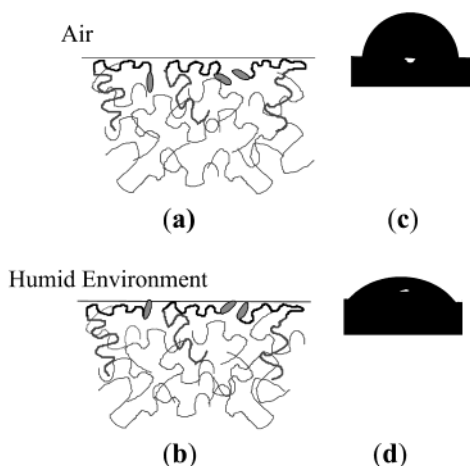


**Figure 1.** Schematic diagram of the methodology employed: When a mixture of X-AB (X is the hydrophilic functional end group) in B is spin coated on a substrate and then annealed above the glass transition temperature, the diblock copolymer partitions to the free surface where the low-energy A block (thick black line) acts as an anchor to the free surface and the B block (thick gray line) forms a dangling chain within the matrix homopolymer (thin gray line). The hydrophilic end group (oval) is brought to the vicinity of the free surface but is hidden below the surface when the specimen is exposed in air (a). When the specimen is exposed to water vapor, the hydrophilic end group responds to the new environment by presenting itself to the surface (b). This reduces significantly the water contact angle with representative drops shown in parts c and d.

collapse of the other.<sup>18</sup> Finally, the surface organization of functional end groups in homopolymers leads to the control of polymer surface properties<sup>19,20</sup> as well as to the modification of polymer/polymer interfaces.<sup>21,22</sup>

Here, we present an investigation on the development of polymer surfaces, which can respond to their environmental conditions. This is demonstrated for surfaces that can alter their wetting characteristics (become hydrophilic) when exposed to water vapor. The methodology proposed utilizes two concepts: the partitioning of an AB block copolymer to the polymer/air interface via its low-energy A block and the surface reorganization of a functional end group X. When an AB diblock copolymer (formed by covalently linking two chemically distinct A and B polymeric chains) is mixed with a B homopolymer, the copolymer partitions to the surface<sup>23,24</sup> with the interfacially active A block acting as an anchor to the surface and the B block (compatible with the homopolymer) forming a dangling chain<sup>25</sup> that keeps the additive tethered to the matrix polymer. This surface partitioning brings a functional (hydrophilic) end group X, chemically attached at the end of the low-energy block, to the vicinity of the surface. The high-energy end group is hidden below the free surface in a dry environment whereas it appears at the surface when exposed to water vapor because of its polarity;<sup>20</sup> this is schematically shown in Figure 1. As a result, the equilibrium contact angle of water is significantly reduced in a switchable way. The end group type, block-length ratio, and additive concentration control the magnitude of the effect. Such a strategy could be used to develop "smart" polymer materials with applications such as wetting, adhesion, and biocompatibility. It is noted that a similar methodology has been proposed<sup>26</sup> to enhance the adhesion selectively toward materials with the proper receptor for the functional moiety.

**Table 1.** Molecular Characteristics of the Samples

code	$M_w^a$	$M_w/M_n^b$	$w_{PI}^c$	end group
NIS-72	24 400	1.07	0.72	dimethylamine <sup>d</sup>
NIS-49	23 500	1.06	0.49	dimethylamine <sup>d</sup>
NIS-31	25 600	1.06	0.31	dimethylamine <sup>d</sup>
NIS-25	20 500	1.07	0.25	dimethylamine <sup>d</sup>
ZIS-72	24 400	1.07	0.72	sulfozwitterion <sup>e</sup>
ZIS-49	23 500	1.06	0.49	sulfozwitterion <sup>e</sup>
ZIS-31	25 600	1.06	0.31	sulfozwitterion <sup>e</sup>
ZIS-25	20 500	1.07	0.25	sulfozwitterion <sup>e</sup>
D-2 <sup>f</sup>	23 300	1.04	0.50	
PS-1	204 000	1.02		
PS-2	9860	1.05		
PSD	190 000	1.04		

<sup>a</sup> Weight-average molecular weight determined by low-angle laser light scattering. <sup>b</sup> The molecular weight polydispersity index determined by size exclusion chromatography. <sup>c</sup> Polyisoprene weight fraction determined by <sup>1</sup>H NMR. <sup>d</sup>  $-\text{CH}_2\text{CH}_2\text{CH}_2\text{N}(\text{CH}_3)_2$ . <sup>e</sup>  $-\text{CH}_2\text{CH}_2\text{CH}_2\text{N}^+(\text{CH}_3)_2\text{CH}_2\text{CH}_2\text{CH}_2\text{SO}_3^-$ . <sup>f</sup> The isoprene block was terminated by methanol; thus, D-2 possesses methyl end groups.

## II. Experimental Section

The copolymer system investigated is polystyrene-*block*-polyisoprene diblocks with two different types of functional groups X at the end of the low-energy polyisoprene block: a dimethylamine and a sulfobetaine (sulfozwitterion) end group (the copolymers are denoted XIS, see Table 1). The end-functionalized diblock copolymers were synthesized by anionic polymerization under high vacuum. The synthesis utilized a 3-(dimethylamino)propyllithium initiator for the introduction of the dimethylamine end group whereas reaction of this group with 1,3-cyclopropane sultone produced the sulfozwitterion moiety.<sup>27</sup> The diblock copolymers were analyzed by size exclusion chromatography using refractive index and UV detection. Weight-average molecular weights were obtained by low-angle laser light scattering whereas the copolymer composition was determined by <sup>1</sup>H NMR spectroscopy. The macromolecular characteristics of the samples are shown in Table 1 together with those of the polystyrene (PS) homopolymers used as the matrix. The diblocks have almost the same molecular weight while their compositions range from 25 to 72 wt % in polyisoprene. The composition of the copolymer, i.e., the relative sizes of the two blocks, is anticipated to influence the tendency for interfacial migration<sup>25</sup> and, thus, the number density of functional groups that may eventually end up at the surface.

Thin films of XIS/PS mixtures (about 300 nm) were spin coated from toluene solutions onto polished and cleaned Si wafers (5 cm in diameter and 5 mm thickness for the neutron reflectivity measurements or 3 cm × 2 cm and 0.5 mm thickness for the contact angle measurements), purchased from Semiconductor Processing Technologies, placed at 60 °C under vacuum to remove the remaining solvent, annealed for 24 h at 170 °C (above the glass transition) in a vacuum to reach equilibrium, and then rapidly quenched to room temperature.

Neutron reflectivity measurements were performed at room temperature at the time-of-flight DESIR reflectometer at the ORPHEE reactor at Laboratoire Leon Brillouin, CEA Saclay, 91191 Gif-sur-Yvette Cedex, France. Deuterated polystyrene PSD (Table 1), with characteristics similar to PS-1, was used as a matrix for these experiments. In brief, a collimated ( $\delta\theta \sim 0.01\text{--}0.03^\circ$ ) neutron beam with a distribution of wavelengths ( $4 < \lambda < 35 \text{ \AA}$ ) impinges upon the specimen surface at a fixed angle  $\theta = 1.8^\circ$  and the reflected intensity is measured also at an angle  $\theta$  with respect to the film surface. The variation of the component of the incident neutron momentum perpendicular to the film surface,  $k_0 = (2\pi/\lambda) \sin \theta$ , is achieved due to the wavelength distribution of the incoming neutron beam. The principles of NR have been discussed previously<sup>28,25</sup> and are not reproduced here, whereas the analysis of the neutron reflectivity data is performed using the matrix method.

The surface tensions of mixtures of polystyrene homopolymer (sample PS-2 with low molecular weight, Table 1) with

the additives against air were measured using the pendant drop method and an automated interfacial tensiometer based on the analysis of axisymmetric fluid drop profiles.<sup>29–31</sup> The method is based on the principle that the shape of the profile of a drop of one fluid into a matrix of another is governed by a force balance between interfacial tension and gravity forces, which is described by the Bashforth–Adams equation. Literature values were used for the calculation of the density of the polystyrene homopolymer,<sup>32</sup> whereas, since the weight fractions of copolymers added is always small (less or equal to 4%), it is assumed that the addition does not affect the density difference across the interface.

The contact angle measurements were performed on thin film specimens, which were prepared as above and then exposed to a saturated water vapor environment for different times in a sealed chamber at 45 °C. They were then removed and the contact angle of Millipore water was measured in air using the automated tensiometer, which utilizes the whole drop profile for the evaluation of both the contact angle and the surface tension of the fluid.<sup>29,33</sup>

X-ray photoelectron spectroscopy measurements were performed in a turbo-pumped UHV chamber equipped with a Leybold LHS-12 hemispherical electron energy analyzer a twin-anode X-ray gun. The unmonochromatized Mg K $\alpha$  line at 1253.6 eV and an analyzer pass energy of 97 eV, giving a fwhm of 1.6 eV for the unresolved Si 2p doublet, were used. Measurements were taken for normal takeoff angle.

### III. Results and Discussion

The free-surface partitioning of the diblocks was verified by surface tension and neutron reflectivity measurements. The surfactant-like character of the diblock copolymers is evident when the surface tension is measured for mixtures of PS with the additives against air using the pendant drop method.<sup>29–31</sup> The surface tension decreases with the additive concentration and reaches a plateau, whereas the values at interfacial saturation are not affected by the type of the functional group,<sup>34</sup> because the group is not exposed right at the surface. Neutron reflectivity investigations of the XIS/PS mixtures quantified the extent of surface partitioning in the films, which depends on additive concentration. Moreover, for the same bulk concentration (e.g., 5 wt %), the diblocks with the sulfozwitterion end group (ZIS) showed a lower adsorbed amount at the air surface than the respective ones with the amine end group (NIS). Since in the absence of a substrate the surface tensions in both cases were the same,<sup>34</sup> this is due to the fact that the sulfozwitterion is strongly attracted to the silicon wafer substrate and, thus, the polymer/substrate interface is enriched in the copolymer as well. This enrichment is less in the case of the dimethylamine end group.

Figure 2a shows the dependence of the equilibrium contact angle of Millipore water on the surface of NIS-31/PS-1 films as a function of the time of exposure to water vapor for various concentrations. The contact angle starts from about 82°, which is between that of pure polystyrene (89°) and pure polyisoprene (79°), for all specimens (a representative drop image is shown in Figure 1c). Following exposure to humid environment the contact angle decreases and reaches values as low as 60°. This is due to the surface reorganization of the amine end groups toward the free surface because they sense the water vapor. The final contact angle decreases when the additive concentration increases from 2 to 5 wt %, whereas no significant difference is observed when the additive concentration increases further to 10 wt %. The kinetics of the surface reorganization depends on concentration in a complicated way, which is not

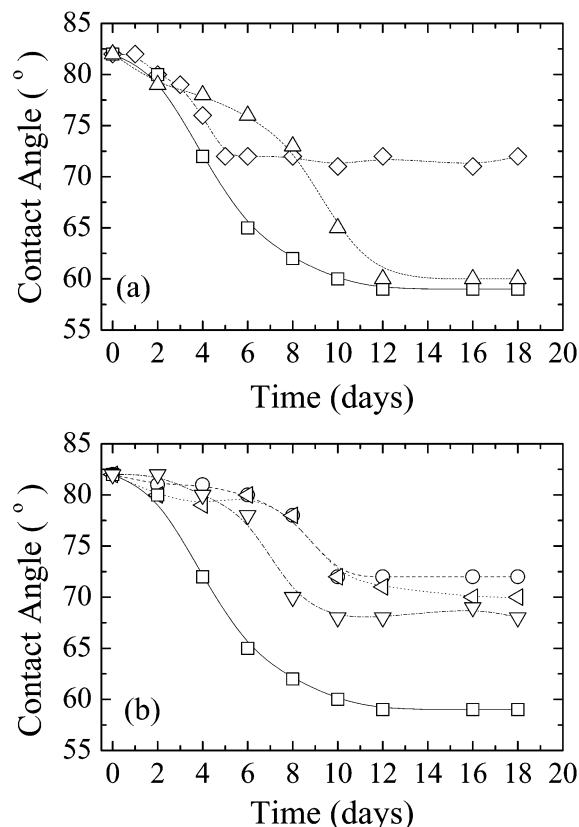


**Figure 2.** (a) Contact angles of NIS-31/PS-1 films vs the exposure time to water vapor for various additive concentrations: 2 wt % ( $\diamond$ ), 5 wt % ( $\triangle$ ), and 10 wt % ( $\square$ ). (b) Contact angles of 5 wt % NIS/PS-1 films vs the exposure time to water vapor for various block-length ratios: NIS-72 ( $\circ$ ), NIS-49 (open triangle pointing left), NIS-31 ( $\square$ ), and NIS-25 ( $\nabla$ ). The best behavior is observed for NIS-31. The error bars are less than the size of the points ( $\pm 1^\circ$ ). The lines are guides to the eye.

understood yet and is under further investigation. For the same additive concentration (5 wt %), the equilibrium contact angle following exposure to water vapor depends on the block-length ratio of the copolymer as can be seen in Figure 2b. The effect is less pronounced for the additive rich in isoprene because there are fewer end groups near the surface. Decreasing the polyisoprene content of the additive (from 72 to 49 to 31%) decreases the final contact angle, because for similar adsorbances there are now more and more end groups near the surface, whereas further decrease to 25% reverses the dependence (the final contact angle for NIS-25 is similar to that for NIS-49). The latter is not understood but, tentatively, it may be due to a lower adsorbance and/or more stable micelles.<sup>36</sup> It should be noted that the contact angles for the respective D-2/PS-1 films (i.e., in the absence of a hydrophilic end group) did not change with exposure time from the initial value of 82° within experimental error.

The effect of the exposure to water vapor is even more pronounced for the ZIS series with the more polar sulfozwitterion end group. Figure 3a shows the dependence of the contact angle on exposure time for films of ZIS-31/PS-1 for various concentrations. The contact angle decreases from about 82° only slightly for concentrations 2 and 5 wt % whereas it shows a dramatic reduction to about 46° for concentration 10 wt % (a representative drop image is shown in Figure 1d). As noted above, neutron reflectivity revealed that, in the



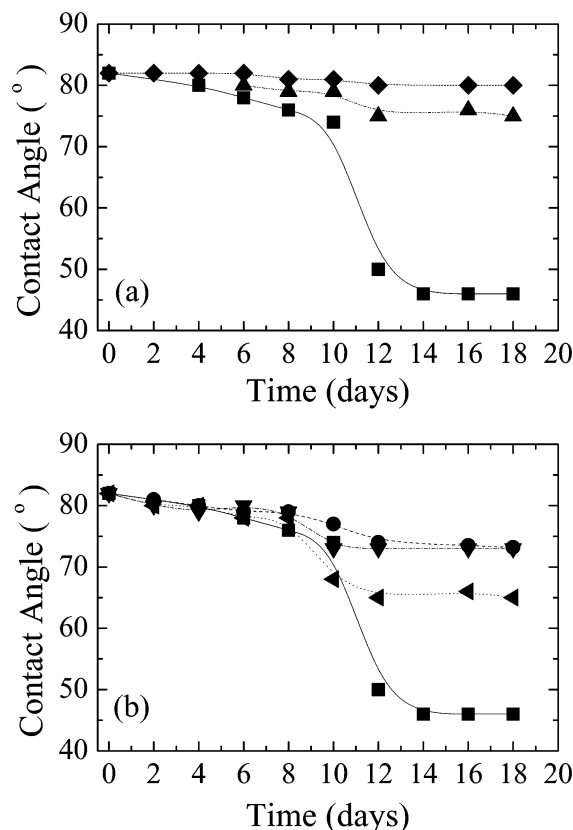


**Figure 3.** (a) Contact angles of ZIS-31/PS-1 films vs the exposure time to water vapor for various additive concentrations: 2 wt % (◆), 5 wt % (▲), and 10 wt % (■). (b) Contact angles of 10 wt % ZIS/PS-1 films vs the exposure time to water vapor for various block-length ratios: ZIS-72 (●), ZIS-49 (solid triangle pointing left), ZIS-31 (■), and ZIS-25 (▼). The optimum behavior is observed for ZIS-31. The error bars are less than the size of the points ( $\pm 1^\circ$ ). The lines are guides to the eye.

case of ZIS, the copolymer partitioning to the free surface is less than that for NIS due to the enhanced segregation of ZIS to the silicon substrate. This is why higher ZIS concentrations are needed (the free surface adsorbance for 5% ZIS-31/PS-1 is even lower than that for 2% NIS-31/PS-1).<sup>35</sup> The achievement of a  $46^\circ$  contact angle with 10 wt % ZIS-31 was the best observed as can be seen in Figure 3b. Similarly to Figure 2b, the additive with 31% polyisoprene was much better than those with either higher or lower polyisoprene fractions for reasons similar to the ones for the NIS series (neutron reflectivity revealed that the adsorbance at the air surface for ZIS-25 was less than for ZIS-31).<sup>35</sup> Something worth noticing is the much more abrupt change in the values of the contact angle after certain exposure times for the ZIS series (Figure 3) than for NIS (Figure 2). It is estimated that this is due to the existence of clusters formed by the zwitterion dipoles;<sup>37</sup> the end groups have to release themselves from these clusters in order to reach the surface. However, this is still a tentative explanation at this time.

It has been, therefore, shown that taking advantage of the surface segregation of diblock copolymers together with the presence of a hydrophilic end group chemically attached at the end of the low surface energy block leads to a surface that can respond to its new environment. In Figure 1, we had schematically presented the surface reorganization that was anticipated in order to obtain the reduction of the contact angle values, which was

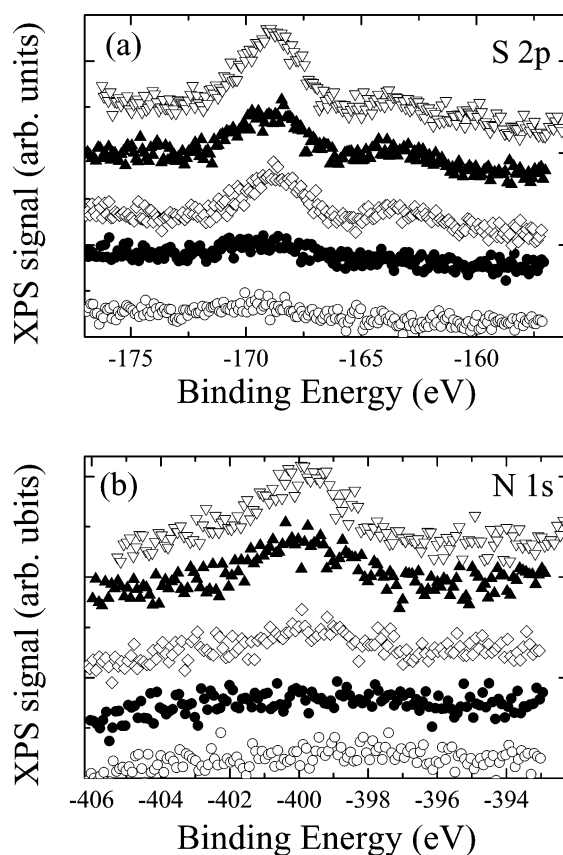


**Figure 4.** X-ray photoelectron spectra (in arbitrary units shifted for clarity) for a 10 wt % ZIS/PS-1 film for various exposure times to water vapor: 1 day (○), 4 days (●), 7 days (◇), 11 days (▲), and 14 days (▼). The spectra are shown in the binding energy range of S 2p (a) and N 1s (b). Between 4 and 7 days of exposure, the nitrogen and sulfur elements of the sulfozwitterion end group appear at the surface.

quantified in Figures 2 and 3. However, one would like to observe whether the schematic presented in Figure 1, parts a and b, is indeed the reason for the reduction of the contact angles from about  $82^\circ$  down to  $46^\circ$ .

X-ray photoelectron spectroscopy (XPS) is a surface-sensitive analytic technique, which can discriminate atoms based on the range of kinetic energies of the emitted photoelectrons originating from core levels. Since the zwitterion end group possesses nitrogen and sulfur atoms, XPS is used to verify the presence (or absence) of the end group in the vicinity of the free surface. Figure 4 shows the photoelectron spectra in the binding energy range of S 2p (Figure 4a) and N 1s (Figure 4b) for films of ZIS-31/PS-1 for various exposure times to water vapor. It is evident that following exposures of 4–7 days, both elements are clearly observed at the surface. Note that the chemical state of the atoms can be detected by XPS because it leads to line shifts: the binding energies associated with both elements agree<sup>38</sup> with the chemical structure of the sulfozwitterion end group. Although the escape depth for X-ray photoelectrons is in the range of 7 nm for polymers, since each end group possesses only one nitrogen and one sulfur atom, their presence is evident only when they are really at the surface.<sup>38</sup> The sulfur to carbon atomic ratio calculated from the photoelectron spectra following 14 days of exposure is found equal to  $1.8 \times 10^{-3}$  compared to about  $5 \times 10^{-4}$  estimated in the bulk; this is roughly the coverage of the sulfur atoms

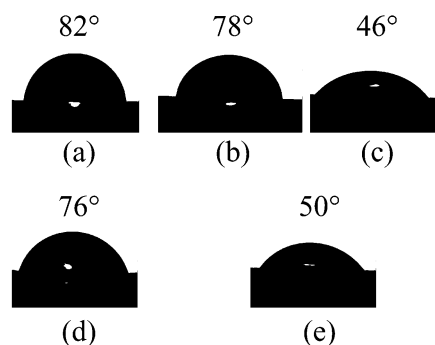


**Figure 5.** “Education” of the smart surface. Representative water drops on a 10 wt % ZIS-31/PS-1 film following (a) no exposure, (b) 5 days exposure to water vapor, (c) 14 days exposure to water vapor, (d) 2 days in a vacuum after (c), and (e) 1 day exposure to water vapor after (d).

(sulfozwitterion end groups) at the vicinity of the free surface. Therefore, XPS clearly verifies the schematic presented in Figure 1.

Finally, the switchability of the behavior was investigated. Figure 5 shows representative drop images for a 10 wt % ZIS-31/PS-1 specimen before exposure (a) and after 5 (b) and 14 days (c) of exposure to water vapor. This is essentially the behavior discussed in relation to Figure 3 above. When the specimen in (c) is held in a vacuum only for 2 days, its contact angle increases already to 76° (d) whereas subsequent exposure to water vapor for only 1 day is enough to reduce the contact angle to 50° (e). This switchable behavior, which does not even require the initial 14 days, can be continued for about five times (on average). This may be an indication that indeed the sulfozwitterion participates at the beginning in some kind of clusters, which slows the reorganization the first time. Subsequently, the zwitterion does not have the time to re-form the clusters, and thus, it switches to and back from the surface faster. Therefore, one can think of “educating” the specimen during the first cycle and following its adaptiveness in the next cycles until it does not function any more.<sup>39</sup>

In summary, we have presented a methodology for the development of smart polymer surfaces, which can respond to changes in their environment. This utilizes a block copolymer with a functional group at the end of the low-surface-energy block. The latter acts as a vehicle bringing the end group to the proximity of the surface whereas by exposing the specimen to water vapor it responds by presenting the hydrophilic end group to the surface. The optimization of the behavior is by no means complete: different end groups, number of end groups per anchor chain, macromolecular architecture will all be important and are under further investigation. This study presents a methodology, which, we believe, can have numerous extensions in the areas of sensors and biomaterials.

**Acknowledgment.** Part of this research was sponsored by NATO’s Scientific Affairs Division (Science for Stability and Science for Peace Programmes) and by the Greek General Secretariat of Research and Technology. We thank H. Watanabe for kindly supplying diblock D-2, K. Hong and J. W. Mays for kindly supplying homopolymer PS-2, A. Menelle for his collaboration in the neutron reflectivity measurements, and G. Fytas, D. Vlassopoulos, K. Chrissopoulou, and M. Vamvakaki for their comments on the manuscript.

## References and Notes

- (1) Koberstein, J. T., Ed. *Polymer Surfaces and Interfaces*. *MRS Bull.* **1996**, 21, 16.
- (2) Bain, C. D.; Evall, J.; Whitesides, G. M. *J. Am. Chem. Soc.* **1989**, 111, 7155.
- (3) Ulman, A. *An Introduction to Ultrathin Organic Films from Langmuir–Blodgett to Self-Assembly*; Academic Press: New York, 1991.
- (4) Mansky, P.; Liu, Y.; Huang, E.; Russell, T. P.; Hawker, C. *Science* **1997**, 275, 1458.
- (5) Genzer, J.; Efimenko, K. *Science* **2000**, 290, 2130.
- (6) Garbassi, F.; Morra, M.; Occhiello, E. *Polymer Surfaces*; John Wiley: New York, 1994.
- (7) Peppas, N. A. *Curr. Opin. Colloid Interface Sci.* **1997**, 2, 531.
- (8) Sato-Matsuo, E.; Tanaka, T. *Nature (London)* **1992**, 358, 482.
- (9) Hu, Z.; Chen, Y.; Wang, C.; Zheng, Y.; Li, Y. *Nature (London)* **1998**, 393, 149.
- (10) Weissman, J. M.; Sunkara, H. B.; Tse, A. S.; Asher, S. A. *Science* **1996**, 274, 959.
- (11) Holtz, J. H.; Asher, S. A. *Nature (London)* **1997**, 389, 829.
- (12) Wang, C.; Stewart, R. J.; Kopecek, J. *Nature (London)* **1999**, 397, 417.
- (13) de Crevoisier, G.; Fabre, P.; Corpart, J.-M.; Leibler, L. *Science* **1999**, 285, 1246.
- (14) Carey, D. H.; Ferguson, G. S. *J. Am. Chem. Soc.* **1996**, 118, 9780.
- (15) Andrade, J. D. *J. Intell. Mater. Syst. Struct.* **1994**, 5, 612.
- (16) Senshu, K.; Yamashita, S.; Ito, M.; Hirao, A.; Nakahama, S. *Langmuir* **1995**, 11, 2293. Senshu, K.; Yamashita, S.; Mori, H.; Ito, M.; Hirao, A.; Nakahama, S. *Langmuir* **1999**, 15, 1754.
- (17) Zhao, B.; Brittain, W. J. *J. Am. Chem. Soc.* **1999**, 121, 3558. Sedjo, R. A.; Miroso, B. K.; Brittain, W. J. *Macromolecules* **2000**, 33, 1492. Zhao, B.; Brittain, W. J.; Zhou, W.; Cheng, S. Z. D. *J. Am. Chem. Soc.* **2000**, 122, 2407.
- (18) Sidorenko, A.; Minko, S.; Schenk-Meuser, K.; Duschner, H.; Stamm, M. *Langmuir* **1999**, 15, 8349. Minko, S.; Usov, D.; Goreschnik, E.; Stamm, M. *Macromol. Rapid Commun.* **2001**, 22, 206. Minko, S.; Patil, S.; Datsyuk, V.; Simon, F.; Eichhorn, K.-J.; Motornov, M.; Usov, D.; Tokarev, I.; Stamm, M. *Langmuir* **2002**, 18, 289.
- (19) Jalbert, C.; Koberstein, J. T.; Hariharan, A.; Kumar, S. K. *Macromolecules* **1997**, 30, 4481.
- (20) Koberstein, J. T. In *Polymer Surfaces, Interfaces, and Thin Films*; Karim, A., Kumar, S., Eds.; World Scientific Pub. Co.: River Edge, NJ, 2000; pp 115–180.
- (21) Fleischer, C. A.; Morales, A.; Koberstein, J. T. *Macromolecules* **1994**, 27, 379.
- (22) Schulze, J. S.; Cernohous, J. J.; Hirao, A.; Lodge, T. P.; Macosco, C. W. *Macromolecules* **2000**, 33, 1191.
- (23) Budkowski, A.; Klein, J.; Fetters, L. J. *Macromolecules* **1995**, 28, 8571.
- (24) Kunz, K.; Anastasiadis, S. H.; Stamm, M.; Schurrat, T.; Rauch, F. *Eur. Phys. J. B* **1999**, 7, 411. Anastasiadis, S. H.; Retsos, H.; Kunz, K.; Toprakcioglu, C.; Smith, G.; Hadziioannou, G.; Gill, R.; Stamm, M. *Polym. Prepr.* **1999**, 40 (2), 116.
- (25) Retsos, H.; Terzis, A. F.; Anastasiadis, S. H.; Anastasiopoulos, D. L.; Toprakcioglu, C.; Theodorou, D. N.; Smith, G. S.; Menelle, A.; Gill, R. E.; Hadziioannou, G.; Gallot, Y. *Macromolecules* **2002**, 35, 1116.
- (26) Koberstein, J. T.; Duch, D. E.; Hu, W.; Lenk, J. T.; Bhatia, R.; Brown, H. R.; Lingelser, J.-P.; Gallot, Y. *J. Adhes.* **1998**, 66, 229.
- (27) Pispas, S.; Hadjichristidis, N. *Macromolecules* **1994**, 27, 1891.
- (28) Russell, T. P. *Mater. Sci. Rep.* **1990**, 5, 171.
- (29) Anastasiadis, S. H.; Chen, J.-K.; Koberstein, J. T.; Siegel, A. F.; Sohn, J. E.; Emerson, J. A. *J. Colloid Interface Sci.* **1987**, 119, 55.
- (30) The instrument described in ref 29 has been commercialized by Materials Interface Associates.
- (31) Retsos, H.; Margiolaki, I.; Messaritaki, A.; Anastasiadis, S. H. *Macromolecules* **2001**, 34, 5295.
- (32) Richardson, M. J.; Savill, N. G. *Polymer* **1977**, 18, 3.
- (33) Anastasiadis, S. H.; Hatzikiriakos, S. G. *J. Rheol.* **1998**, 42, 795.
- (34) The surface tension of PS/additive mixtures was measured at 140 °C using a low molecular weight polystyrene homopolymer (PS-2) as the matrix. The surface tension of PS-2 is 30.8 ± 0.3 mN/m, whereas the surface tensions at interfacial saturation of the mixtures are 27.2 ± 0.2 mN/m for PS-2/

- D-2 (with methyl end groups),  $27.1 \pm 0.2$  mN/m for PS-2/NIS-31, and  $27.2 \pm 0.3$  mN/m for PS-2/ZIS-31.
- (35) Adsorbed amounts for the copolymer at the free surface can be calculated from the scattering length density profiles obtained from the analysis of the neutron reflectivity data (eqs 2–7 of ref 25). Although the errors introduced by the present deuteration scheme are large,<sup>25</sup> these adsorbed amounts  $z^*$  are 7 nm for 2 wt % of NIS-31, 17 nm for 5 wt % of NIS-31, 6 nm for 5 wt % of ZIS-31, 8 nm for 10 wt % of ZIS-31, and 7 nm for 10 wt % of ZIS-25.
- (36) For the molecular weights and the concentrations used in the present work, a calculation for the critical micelle concentration based on the theoretical expressions for the chemical potentials used in ref 31 and neglecting the effects of the end groups (amine and sulfonwitterionic) indicates that micelles will not be present for NIS-31, NIS-25, ZIS-31, and ZIS-25 whereas they will be present for NIS-49, NIS-72, ZIS-49, and ZIS-72. The work of ref 31 pointed out at the importance of micellization on interfacial partitioning.
- (37) Hadjichristidis, N.; Pispas, S.; Pitsikalis, M. *Prog. Polym. Sci.* **1999**, *24*, 875.
- (38) *Practical Surface Analysis*, 2nd ed.; Briggs, D., Seah, M. P., Eds.; John Wiley & Sons: Ltd.: West Sussex, England, 1996; Vol. 1.
- (39) Following extensive exposure to water vapor (20 and 25 days), a second peak appears in the S 2p binding energy range at about 162 eV, which corresponds to elemental sulfur probably due to surface contamination or decomposition of the sulfonwitterion. At the same time, the N 1s peak becomes very broad and weak.

MA0211129